PHYSICAL REVIEW B VOLUME 57, NUMBER 4 15 JANUARY 1998-II

ARTICLES

Theoretical investigation of the high-pressure phases of Ce

P. Ravindran, L. Nordström, and R. Ahuja
Condensed Matter Theory Group, Department of Physics, Uppsala University, Box 530, 75121 Uppsala, Sweden

J. M. Wills
Center for Materials Science and Theoretical Division, Los Alamos National Laboratory, Los Alamos, New Mexico 87545

B. Johansson
Condensed Matter Theory Group, Department of Physics, Uppsala University, Box 530, 75121 Uppsala, Sweden

O. Eriksson
Condensed Matter Theory Group, Department of Physics, Uppsala University, Box 530, 75121 Uppsala, Sweden
and Center for Materials Science and Theoretical Division, Los Alamos National Laboratory, Los Alamos, New Mexico 87545

(Received 16 June 1997)

In order to shed light on the recent experimental controversy concerning the intermediate pressure phases of Ce we have made systematic electronic structure and total-energy studies on Ce in the experimentally reported low-pressure phase α-Ce (fcc), the intermediate-pressure α-U (α'), the body-centered monoclinic [α''(I)], and C-face-centered monoclinic [α''(II)] phases, together with the stable high-pressure body-centered tetragonal phase. We also included the body-centered cubic, hexagonal-close-packed, and ω ($hP3$) phases. In this study we used the accurate full-potential linear muffin-tin orbital (FPLMTO) method. The optimized structural parameters obtained from our total-energy studies for the α' and α''(II) phases are found to be in good agreement with corresponding experimental values. The structural optimization of the α''(I) phase always yields the fcc or bct phase stable, depending upon the volume considered. Except for an improvement in the equilibrium volume, the generalized gradient correction reproduces the calculated relative stability between different phases of Ce at high pressure of the local-density approximation. Of the experimentally reported intermediate pressure structures [α', α''(I) and α''(II)] we find that the α''(II) phase is the most stable. Among the contending phases, α' and α''(I), the latter is very close in energy to the α'' phase whereas the former is substantially higher in energy. We thus rule out the α-U structure as an intermediate pressure phase of Ce. Our work suggests that the most probable structural phase transition sequence of Ce metal is fcc(γ)$\rightarrow$fcc(α)$\rightarrow$ α''(II) $\rightarrow$ bct, which is consistent with current experimental results.
[S0163-1829(98)03004-5]

I. INTRODUCTION

Since Bridgeman's[1] discovery of the fcc isostructural $\gamma \rightarrow \alpha$ transition in Ce in 1927, this metal has been studied extensively both experimentally and theoretically. Under various conditions of temperature and pressure, cerium is an antiferromagnet, a superconductor, and the only pure element to exhibit a pressure-induced isostructural transition. It is the first lanthanide metal that has an appreciable occupation of the $4f$ states, and is a known subject for controversy concerning the electronic structure. Primarily the debate concerns the localized versus itinerant nature of the $4f$ electrons.

There are four allotropic forms of Ce at ambient pressures; the bcc δ phase, a dhcp β phase, an fcc γ phase, and an fcc α phase.[2] The first-order $\gamma \rightarrow \alpha$ transition with a volume collapse of $\sim 16\%$, that occurs at 116 K at ambient pressure or at 0.7 GPa at 298 K (Ref. 3) has been extensively studied both experimentally and theoretically. Several models explaining the unusual $\gamma \rightarrow \alpha$ transition have been proposed such as the promotional model (PM),[4] the Kondo volume collapse (KVC) model,[5] the Mott transition model[6] (MT) and lately a model by Sandalov *et al.*[7] based on strong-coupling theory. Neither band- structure calculations[8,9] based on local-density approximations nor photoemission studies[10] have been able to confirm the PM. More importantly the PM is inconsistent with the observed cohesive energy of Ce.[6] In the KVC model the transition is assumed to be governed by Kondo screening of the spin of the localized f electron by the delocalized (spd) conduction electrons. The $4f$ electrons are assumed to be magnetic localized in both α-Ce and γ-Ce, but the effectiveness of the Kondo screening is different in the two phases. This screening is well established for an isolated localized moment,[11] but until now the exact solution of a Kondo Hamiltonian for a periodic array of local moments interacting with conduction-band states has not been found in three dimensions. The MT model[6] considers the f states to be itinerant and bonding for α-Ce, but localized (magnetic) and nonbonding for γ-Ce. The localization

0163-1829/98/57(4)/2091(11)/$15.00

of f states in the γ phase is driven by the large on-site f-f Coulomb interaction dominating over the f-band energies. When the volume is decreased the f-f and f-(spd) hopping integral increases and eventually the band formation energy gained by building Bloch states outweights the increase in Coulomb energy. Calculations of Boring *et al.*,[12] which included Hubbard-Kanamori interactions as proposed by Brandow[13] (the so called LDA+U approach), supported the MT model showing that the U necessary to localize the $4f$ states of Ce is much larger than the $4f$ bandwidth. Similar results were obtained by Sandalov *et al.*[7] Self-interaction corrected local spin density calculations,[14] and band structure calculations[8,9] also suggest that the $\gamma \rightarrow \alpha$ transition is a Mott type transition of the $4f$ electrons. Recently, on the basis of the Mott transition model, density functional (DF) calculations were carried out that correctly described the topology of the experimentally observed phase diagram.[15]

Similar to the γ-Ce(fcc)$\rightarrow \alpha$-Ce(fcc) transition much effort has been directed to determine the phase to which α-Ce transforms at 5 GPa. The high-pressure phase above 5 GPa for Ce was first observed by Wittig[16] from high-pressure electrical resistivity measurements. He detected superconductivity with a transition temperature of 1.3 K in this phase. He also observed that the 5 GPa phase transition is sluggish at room temperature. Following this Franseschi and Olcese[17] made high-pressure x-ray diffraction analysis and found a 4% volume collapse at the 5 GPa structural transition. They interpreted this new phase as a ‘‘strongly collapsed’’ tetravalent phase. From the *in situ* x-ray diffraction measurements McWhan[18] suggested that Ce stabilizes in the hcp structure (like tetravalent Ti and Zr) above 5 GPa. Ellinger and Zachariasen[19] reported an α-U type orthorhombic structure (α') for Ce above 5.6 GPa. Moreover, a body centered monoclinic structure [α''(I) with space group I2/m] has been observed above 6 GPa.

From *in situ* x-ray diffraction measurements on high-purity Ce, Schaufelberger[20] reported that Ce exhibits an fcc → hcp structural transformation at 5.1 GPa with a ~7% volume collapse. Later Endo, Sasaki, and Mitsui[21] reported a new allotropic phase for Ce with a bct structure above 12.1 GPa. Zachariasen and Ellinger[22] found a mixture of α' and α''(I) phases for pressures above 5 GPa and they have claimed that the α' phase is the stable phase and the α''(I) phase is the metastable phase for Ce in this pressure range. Zachariasen interpreted[23] the *in situ* x-ray diffraction data reported by Endo, Sasaki, and Mitsui[21] around 5–10 GPa as a distorted fcc structure called α''(II) with space group $C2/m$. Olsen *et al.*[24] found an α(fcc)$\rightarrow \alpha''$(I) phase transition at 5 GPa and an α''(I) → bct phase transition at 12 GPa from high-pressure x-ray diffraction measurements. They found no evidence of the $\alpha'(\alpha$-$U)$ structure. Sikka and Vijayakumar suggested[25] that if one relaxes the atom position parameter y in the α''(II) structure another monoclinic structure with space group $P2_1/c$ will emerge, which may be stable in Ce at elevated pressures.

Recently Gu, Vohra, and Brister[26] investigated crystal structure and orientation effects in Ce up to 28 GPa at room temperature by high-resolution synchrotron x-ray diffraction using an image plate technique with a diamond anvil cell and observed crystal grain growth during the phase transformation to the $\alpha'(\alpha$-$U)$ structure at high pressures. They also reported that the $\alpha'(\alpha$-$U)$ phase is the stable phase of Ce between 5 and 13 GPa at room temperature, while the stability range of the body-centered monoclinic phase [α''(I)] is limited to between 5 and 7 GPa. Very recent angle dispersive powder diffraction measurements[27] as a function of temperature and pressure suggest that Ce is stable in the C-face-centered monoclinic [fcm, α''(II)] structure with symmetry $C2/m$) at room temperature in the pressure range ~5GPa to 12 GPa. Above 100 °C the experiments of Zhao and Holtzapfel[28] yield the α-U phase. Zhao and Holzapfel[28] made energy dispersive x-ray diffraction studies on Ce at pressures up to 14 GPa and temperatures up to 625 K. They concluded that the $\alpha'(\alpha$-$U)$ + α''(I) (bcm) phase mixture is stable above 4 GPa and low temperature while the pure α' (α-U) phase is stable above 400 K.

From this review of experimental results it is clear that the crystal structure data in the high-pressure region between 5 to 12 GPa are confusing and contain contradictions. However, we also note that there is no dispute between different experimental studies regarding the stability of the bct phase above 12 GPa. In order to clarify the issue at the intermediate pressures detailed total-energy studies on the relative stability between the experimentally reported various structures would be helpful and this is the main motivation of the present study.

One particular reason for trying to understand the complex structural properties of Ce metal is that indirectly the atomic arrangement gives information about the nature of the $4f$ electrons, a much debated issue. In particular, it is expected that the similarity between the high-pressure structures in Ce metal and the light actinide metals is a strong indication that the nature of the f electrons is also similar.[6] This suggests delocalized $4f$ states in the high-pressure phases of Ce metal and also in the ambient condition, α-Ce phase. Skriver[29] and subsequently Wills *et al.*[9] supported this idea by theoretical calculations where the $4f$ states were treated as itinerant, which gave good agreement concerning the suggested α to α' (α-U) and the α' to bct structural sequences. In the work of Wills *et al.*[9] this sequence was explained to be a balance between the $4f$ band states, which due to Peierls/Jahn-Teller–like symmetry breaking mechanisms favor distorted structures, and electrostatic interactions, which favor high-symmetry structures. With the new experimental debate concerning whether or not it is the α-U structure which is the correct intermediate pressure structure, or if it is the $C2/m$, $I2/m$ or $P2_1/c$ structures, we have undertaken a thorough theoretical investigation of the various proposed high-pressure phases of Ce metal.

The rest of this paper is organized as follows. The computational details used in the present calculations are given in Sec. II. Section III deals with the structural relation between various high-pressure phases of Ce. The results obtained from our electronic-structure and total-energy studies are given in Sec. IV, where they are compared with experimental results. The important conclusions arrived from our theoretical studies are given in the last section.

II. COMPUTATIONAL DETAILS

As the earlier electronic structure studies[9,29] have shown, the high-pressure phases of Ce—including the α phase—

have itinerant $4f$ electrons. Accordingly, we have treated the $4f$ states of Ce as itinerant (Bloch) states in all our calculations. The present *ab initio* method solves the Dirac equation (for the core electrons) or a (modified) Schrödinger equation (for the valence and semicore electrons) in the framework of the linear muffin-tin orbital (LMTO) method. The total energy of the system was obtained using the local-density approximation to density-functional theory. The relativistic effects are included in the Hamiltonian. In the semicore and valence electrons the spin-orbit interaction term is considered according to the recipe proposed by Andersen.[30] The wave functions are expanded by means of linear muffin-tin orbitals with a so-called double basis set. We allow two tails with different kinetic energy for each muffin-tin orbital with a given l-quantum number. The calculations were done for one, fully hybridizing energy panel in which the linearization energies both for the valence orbitals $6s$, $6p$, $5d$, and $4f$, and for the semicore orbitals $5s$ and $5p$ were defined. Within the muffin-tin spheres, the basis functions, charge density, and potential were expanded in spherical harmonics with a cutoff $l_{\max}=8$. Outside the muffin-tin spheres, in the interstitial region, the wave functions are Hankel or Neumann functions that are represented by a Fourier series using reciprocal lattice vectors. This treatment of the wave function, charge density, and potential does not rely upon any geometrical approximations and the described type of computational method is usually referred to as a full-potential linear muffin-tin orbital method (FP-LMTO). This full-potential method[31] has previously been successfully applied to many systems, including also structural studies of some of the actinides,[32] proving its reliability. The sampling of the k points in the irreducible part of the first Brillouin zone (IBZ) is done using the special k point method.[33]

There are no standard translational vectors available for the body centered monoclinic lattice. We have used the following translational vectors for our α''(I) phase total-energy studies.

$$T=1/2\begin{pmatrix} a\ \sin(\beta) & b & c+a\ \cos(\beta) \\ -a\ \sin(\beta) & -b & c-a\ \cos(\beta) \\ a\ \sin(\beta) & -b & -[c-a\ \cos(\beta)] \end{pmatrix}.$$

The advantages for using the above translational vectors are as follows.

1. If $\beta=90°$ the translational vectors correspond to the body-centered orthorhombic lattice.

2. If $\beta=90°$ and $a=b$ one obtains the bct translational vectors.

3. If $\beta=90°$ $a=b$ and $c/a=\sqrt{2}$, it is equivalent to the fcc lattice.

4. If $\beta=90°$ $a=b=c$, the translational vectors correspond to the bcc lattice.

Hence by optimization of the structural parameters; β, a/b and c/b, one can arrive at the fcc, bct, bcc, bco, or body-centered monoclinic lattices, depending on the structural parameters.

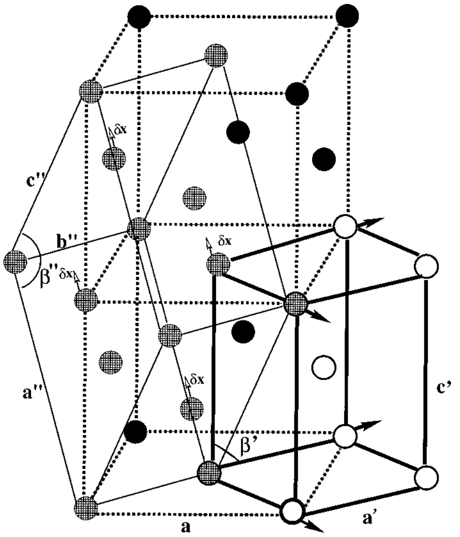

FIG. 1. The relationship between the face-centered cubic (dotted lines with black circles—main cell), body centered tetragonal/monoclinic (bold line subcell with unfilled circles) and the C-face-centered monoclinic (thin line subcell with hatched circles) structures. For more details about the relationship between these structures see Table I.

III. STRUCTURAL RELATIONS

The structural relationship between the fcc, $C2/m$, and bct structures are shown in Fig. 1. The optimized structural parameters for these three structures in terms of the $C2/m$ Bravais lattice is given in Table I. The C-face-centered layers in this structure can be seen to correspond to the close-packed (111) planes of the fcc structure and the δx displacements lie in these planes. The $C2/m$ structure is considered to be a slightly distorted version of the fcc structure. At a volume of 19.7 Å^3/atom, each Ce atom in the fcc structure is surrounded by 12 Ce atoms as neighbors at a distance of 3.0315 Å. In the $C2/m$ structure (at the same volume) with the structural parameters given in Table I, each Ce atom is surrounded by one atom at 2.7978 Å, two atoms at 2.9602, two atoms at 2.9789 Å, four atoms at 3.0676 Å, two atoms at 3.1734 Å and one atom at 3.1983 Å. In the bct structure (again at the same volume), with $c/a=1.6697$, each Ce is surrounded by 4 Ce at 2.8681 Å and 8 Ce at 3.1389 Å. For the same volume, in the α-U structure with the optimized structural parameters, as calculated in Fig. 2 each Ce atom has two neighbors at 2.7138 Å, two at 2.8776 Å, four at 3.1457 Å and four Ce neighbors at 3.2692 Å. Compared with the fcc structure, this shows that the atomic displacement in

TABLE I. The structural parameters for the fcc, bct, and $C2/m$ phases of Ce in the common $C2/m$ lattice.

Parameter	fcc	$C2/m$	bct
x	0.25	0.2618	0.25
z	0.25	0.2517	0.25
β	109.4712°	112.351°	118.1652°
a/b	1.7320	1.8150	1.9462
c/b	1.7320	1.8087	1.9462

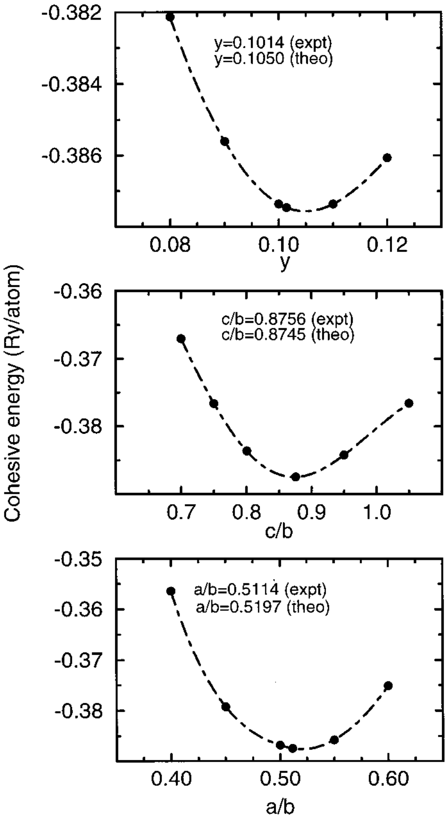

FIG. 2. Calculated total-energy curves for Ce in the α-U structure as a function of structural parameters at the volume 19.7 Å^3/atom. The experimental values are taken from McMahon and Nelmes (Ref. 27).

the α-U structure is larger than in the $C2/m$ structure.

Our structural optimization curves for the $C2/m$ structure is given in Fig. 3, and this figure shows that apart from the displacement of atoms (with respect to fcc) along x ($\delta x = 0.0147$) indicated by arrows in Fig. 1, a finite atom displacement is present along the z axis ($\delta z = 0.00408$) as well. As mentioned earlier, if we relax the y position of Ce in the $C2/m$ lattice, one will arrive at a $P2_1/c$ lattice. But, the structural optimization of the $P2_1/c$ structure, given in Fig. 4, shows that the atoms are not displaced along the y axis in the $C2/m$ lattice. Theory thus rules out the $P2_1/c$ structure. The fcc structure can be described as a bct structure with $c/a = \sqrt{2}$. The experimentally often observed body-centered monoclinic structure can be viewed as a small monoclinic distortion of the bct lattice. That is, by a small elongation along a' and a small distortion of β ($\beta' \approx 90°$) one can describe the monoclinic lattice. However, our structural optimizations of the body-centered monoclinic lattice (see Fig. 5) always gives $\beta' = 90°$ irrespective of the volume we have considered. This result indicates the low possibility for Ce to stabilize in the body-centered monoclinic structure at high pressures.

The finite atom displacements, present in the intermediate pressure phases $C2/m$ and α-U, become zero at the transition to the body-centered tetragonal cell (bold lined cell in Fig.1) with $\beta' = 90°$ and $c'/a' = 1.6697$. As the fcc, $C2/m$ and bct structures are closely related to each other (see Table I), the fcc$\rightarrow C2/m \rightarrow$bct structural sequence is quite possible on geometrical grounds.

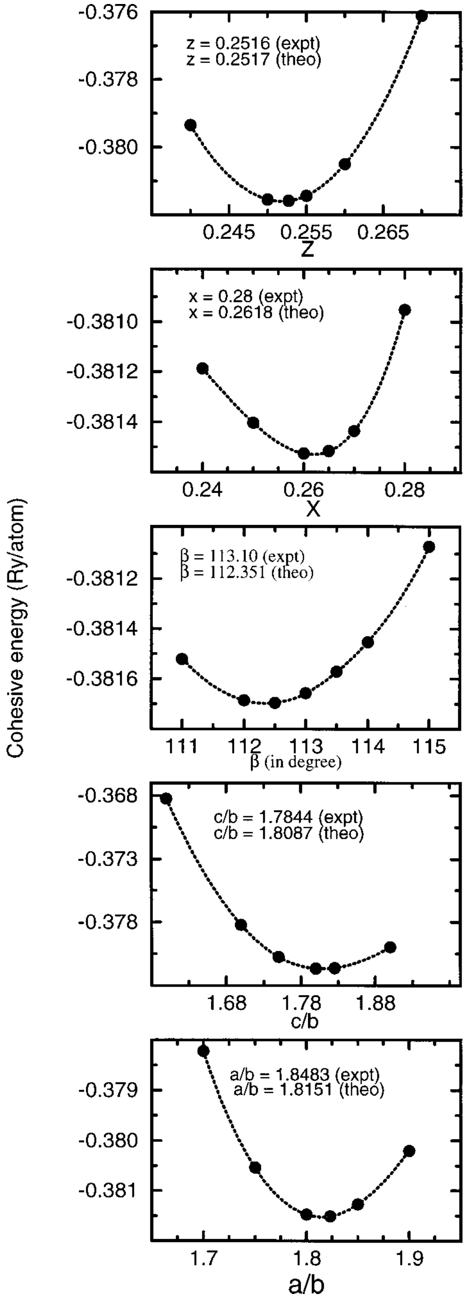

FIG. 3. Calculated total-energy curves for Ce as a function of structural parameters in the $C2/m$ structure at the volume 19.7 Å^3/atom. The experimental parameters are taken from McMahon and Nelmes (Ref. 27).

IV. RESULTS AND DISCUSSIONS

A. Structural stability of possible high-pressure phases

In order to get an idea about the relative stability between the various experimentally reported high-pressure crystal structures of Ce, we started our study by performing a set of calculations (SET1) using the experimental structural parameters; i.e., we did not try to optimize the structural parameters. Furthermore, we also considered the possibility that Ce is tetravalent at high pressure in the same sense as titanium

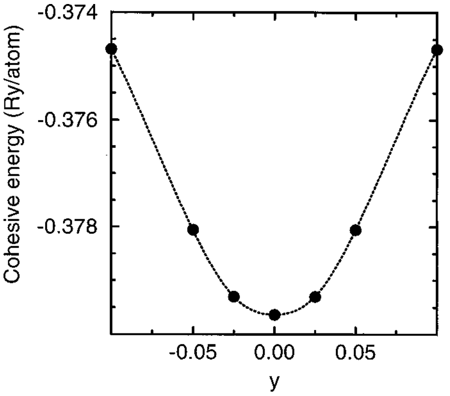

FIG. 4. The total-energy curve for Ce in the $P2_1/c$ lattice as a function of the atomic position parameter y, at the volume 19.7 Å^3/atom.

and zirconium. With such an assumption one would expect a hcp$\rightarrow\omega\rightarrow$bcc structural transition sequence. Accordingly, it is interesting to establish the relative stability between the fcc, hcp and the ω phases under pressure. In these calculations we have used 72 k points for the fcc ($cF4$), 63 k points for the C face centered monoclinic ($mC4$), 59 k points for bct ($tI2$), 68 k points for α-U phase ($oC4$), 80 k points for the body-centered monoclinic ($mI2$), 84 k points for bcc ($cI2$), 65 k points for the hexagonal close-packed ($hP2$) and 50 k points for the ω phase ($hP3$)in the irreducible part of the Brillouin zone (IBZ). For the α-U structure we used $a/b=0.5115$, $c/b=0.8756$ and the atomic position parameter $y=0.1015$ as obtained from the recent high-temperature, high-pressure studies by McMahon and Nelmes.[27] For the α''(II) phase we have used $a/b=1.8483$, $c/b=1.7844$, and $\beta=113.10°$ and the atomic positional parameters $x=0.28$ and $z=0.2517$ were taken from the recent low-temperature, high-pressure measurements.[27] For the α'(I) phase we used $a/b=0.9880$, $c/b=1.5121$, and $\beta=91.92°$ as obtained from the recent high-pressure synchrotron x-ray diffraction studies of Gu, Vohra, and Brister.[26] For the hexagonal phases we used $c/a=1.64556$ for the close-packed hexagonal phase taken from the experimental value given by McWhan[18] and the standard value of $c/a=0.625$ for the ω phase.[34]

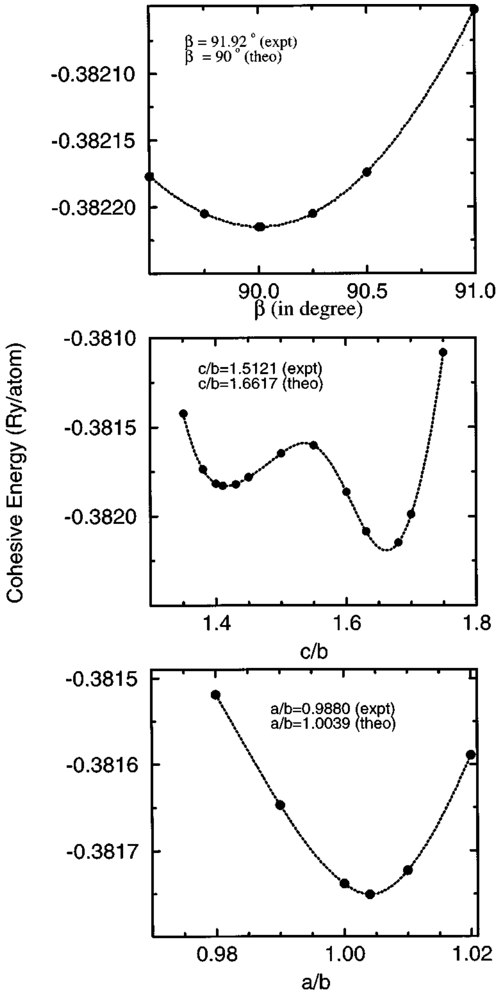

FIG. 5. The total-energy curves for Ce in the body-centered monoclinic structure as a function of a/b, c/b, and angle β at the volume 19.7 Å^3/atom. The experimental values are taken from Gu, Vohra, and Brister (Ref. 26).

Among the experimentally reported high-pressure phases we find that the α, α''(I), and α''(II), and bct are very much closer in energy to each other than the other structures in Fig. 6. At lower volumes, the energy differences between the α, α''(I), α''(II) structures are very small. However, the $\alpha\rightarrow$ bct structural transition is only obtained at a volume of 20.2 Å^3/atom. All the other phases are higher in energy. This is in agreement with the calculations of Wills, Eriksson, and Boring.[9] In a small volume interval around 19 Å^3 we calculate that the fcc, bct, $mC4$, and $mI2$ structures lie within a fraction of a mRy of each other. Unfortunately this is smaller than the accuracy of our calculations and it is hard from theory to favor one of the intermediate pressure phases over the others. On the other hand, since the α-U and hcp structures are higher in energy for all volumes we can rule out their existence as ground-state allotropes for pressure within 1 Mbar. This is in disagreement with the calculations of Wills *et al.*,[9] who found the α-U structure to be stable in a

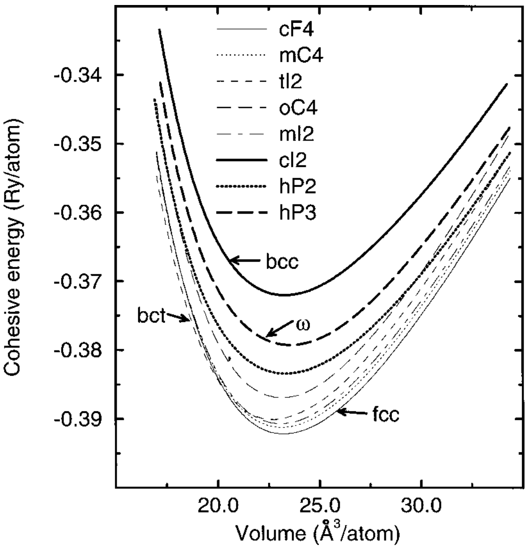

FIG. 6. Calculated binding energy curves for Ce in the fcc ($cF4$), C-face-centered monoclinic ($mC4$-$C2/m$), bct ($tI2$), α-U ($oC4$), body-centered monoclinic ($mI2$), bcc ($cI2$), hcp ($hP2$), and ω phase ($hP3$) structures as a function of atomic volume.

small pressure range. This result is due to the fact that they used a smaller basis set and a lower number of k points. Keeping the accuracy of our method in mind (we believe that we have an energy resolution of approximately 0.5 mRy when we consider structural aspects). We notice that our results in Fig. 6 are consistent with the experiments of Refs. 21 and 24.

It is fully logical to expect that if the $4f$ levels no longer will be populated (i.e., if one assumes the validity of the promotion model) Ce should behave like Ti, Zr, or Hf, which show the hcp structure at ambient pressure and low temperature. Ti, Zr, and Hf are all different from other transition-metal elements as regards the stability of the ω phase (hexagonal phase with three atoms/unit cell, AlB_2 type) at high pressure. Hence if the f electrons were not participating in the bonding one would expect the ω phase to be stable at high pressure also for Ce. Interestingly, the ω phase is found to be much higher in energy than all the experimentally reported high pressure phases considered in Fig. 6. This demonstrates clearly the importance of the f electrons for the metallic bonding and the structural behavior of Ce at high pressures. The same conclusion can be drawn from the observations of distorted structures in this metal. In this respect the present results fully support the view of f bonding put forward by Johansson[6] and they also confirm the earlier results obtained by Wills, Eriksson, and Boring.[9]

B. Structural optimization of the experimentally reported high-pressure phases of Ce

In a second set of calculations, SET2, we have performed structural optimizations for the experimentally reported high-pressure phases of Ce. Thus, for the α' phase we have optimized the structural parameters a/b, c/b and the atom position parameter y (at the volume 19.7 Å^3/atom using 150 k points in the IBZ). Similarly for the α''(I) phase we have optimized the structural parameters a/b, c/b, and β at the volumes 22, 19.7 and 18 Å^3/atom (using 150 k points in the IBZ of the body-centered monoclinic lattice). In the case of the α''(II) phase we have optimized the structural parameters a/b, c/b, β, and the atom positional parameters x and z at the volumes 22 and 19.7 Å^3/atom (using 150 k points in the IBZ of the C-face-centered monoclinic lattice). Further, in order to elucidate the physical origin of the high-pressure metastable phase, we have calculated the total energy as a function of c/a for the bct structure. This was done for eight different volumes with 163 k points in the IBZ of the bct lattice. The total-energy change as a function of the c/a ratio is very small and hence we have continued the self-consistent iterations until the total-energy difference between two consecutive iterations was less than 1 μRy. As discussed by Sikka and Vijayakumar,[25] if one relaxes the internal parameter y in the $C2/m$ lattice one will arrive at a primitive monoclinic lattice of space group $P2_1/c$ with 4 atoms/cell. In accordance with this we have fixed all the structural parameters, such as a/b, c/b, β, x and z of the $C2/m$ lattice obtained from our structural optimization and used these data for the $P2_1/c$ lattice and then relaxed the y parameter of this structure using 108 k points in the IBZ of the primitive monoclinic lattice.

The calculated structural optimization curves for Ce in the α-U structure at the volume 19.7 Å^3/atom are shown in Fig. 2. The position parameter y obtained from our structural optimization is found to be in excellent agreement with that of Skriver[29] and in fair agreement with that of Wills, Eriksson, and Boring from total-energy studies on Ce.[9] However, it differs slightly from the value of 0.1014(2) obtained in the most recent high-pressure experimental study at high temperature.[27] The calculated c/b as well as a/b axis ratios are found to be in very good agreement with the experimental data. This demonstrates that, although LDA underestimates the equilibrium volumes by 5–10 %, it reproduces the internal structural parameters very well. Again this confirms the picture of itinerant $4f$ states in these crystal structures.

The structural optimization curves for the α''(I) phase are shown in Fig. 5. From this figure it is clear that the monoclinic distortion is not favorable in this phase. In order to investigate the role of the volume on the monoclinic distortion we have optimized the β value for different densities and always found that $\beta=90°$ gives the minimum-energy configuration for all volumes. The c/b optimization yields a value of $\sqrt{2}$ (equivalent to fcc) at higher volumes and 1.6617 (equivalent to bct) at lower volumes.

If the atom positions for the $C2/m$ phase are undistorted from the fcc structure, the atomic position parameters x and z will be 0.25. The calculated optimized position parameters given in Fig. 3 clearly show that a finite atom displacement away from the fcc phase is energetically more favorable, i.e., the $C2/m$ structure is more stable than the fcc structure. As both the $x$and z atom positions are considerably displaced in the $C2/m$ structure, one may expect a displacement of the y parameter as well. However, the optimized y parameter for the $P2_1/c$ structure given in Fig. 4 clearly shows that the displacement along y in the $C2/m$ structure is not possible energetically. Further, the optimized β value for the $C2/m$ lattice given in Fig. 3 deviates from the value of the fcc structure $[\cos^{-1}(-1/3)]$ and this indicates that some monoclinic distortion is energetically favorable. In order to investigate the volume effect on the structural parameters of Ce in the $C2/m$ structure we have also optimized all the five structural parameters at a larger volume (22.0 Å^3/atom). Within the accuracy of our calculations, the structural parameters obtained from the different volumes do not change considerably. It should be noted that overall the theoretically obtained structural parameters are found to be in good agreement with the recent experimental values.[27] This once again proves the reliability of full-potential LDA calculations when predicting structural parameters for complicated structures.

The calculated Bains path is shown in Fig. 7 as a function of volume. These paths show that there are two prominent minima as a function of c/a, one at $c/a=\sqrt{2}$ (corresponding to the fcc structure) and another at $c/a\approx1.6697$ (corresponding to the optimized bct structure). Another interesting aspect of these Bains paths is the appearance of a local minima between $c/a=\sqrt{2}$ and 1.6697 for a certain range of volumes (19–20 Å^3/atom). We have found that this local minimum appears at $c/a=1.5079$ and that the corresponding c/b in the $C2/m$ lattice is 1.8093. This c/b value is found to be in very good agreement with the $c/b=1.8087$ obtained from the structural optimization of the $C2/m$ structure given in Fig. 3.

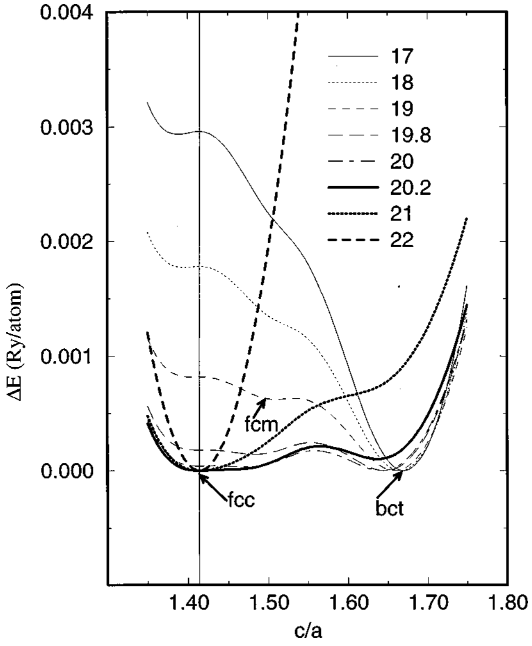

FIG. 7. The Bains path for the fcc→bct structural transition. The minima at $\sqrt{2}$ corresponds to the fcc structure, 1.508 is related to the $C2/m$ (fcm) structure, and 1.67 corresponds to bct structure. For each curve the global minimum is set equal to zero.The vertical line corresponds the c/a for the fcc structure.

This confirms the possibility of stabilizing the $C2/m$ structure for Ce in an intermediate pressure range. However, the minimum corresponding to the $C2/m$ structure is always higher in energy than that of the fcc or bct structure. This suggests that the $C2/m$ phase must be metastable. If, instead of optimizing the crystal parameters in a narrow range around the experimental data, we would have performed a global optimization the fcc or bct structures would have been retained. Therefore the experimentally observed high-pressure $C2/m$ phase in the range 5–11 GPa is of a metastable type and may be stabilized by impurities, temperature, pressure history of the sample, etc. The c/a variation as a function of volume is shown in Fig. 8. It can be seen that the equilibrium c/a for the bct structure is only weakly dependent on pressure and this is consistent with the experimental studies.[28,24,21] The appearance of local minimum between $c/a=\sqrt{2}$ (fcc) and 1.6697 (bct) in Fig. 7 indicates that the pressure induced structural transition is not a simple mechanism of a pure shear distortion (Bain mechanism). Our structural optimizations of the α' and α''(II) structures show that the atoms are displaced considerably from the fcc phase in this high-pressure phase. Hence, instead of a pure shear distortion from the fcc phase the intermediate pressure structural transformation appears to involve a combined shear and layer shuffling (Burgers mechanism).

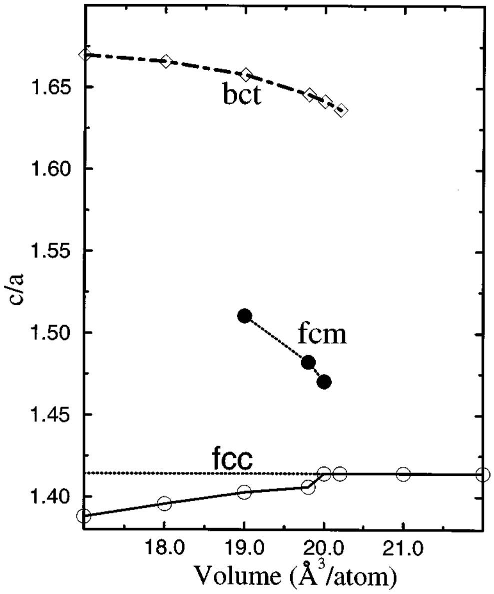

FIG. 8. The variation of c/a as a function of volume for Ce in the fcc, fcm, and bct structures.

As a final remark in this section we would like to emphasize that our calculations show that the energy differences between some of the suggested high pressure phases of Ce are of the order of 0.1 mRy, which unfortunately is just on the border of our energy resolution. In Sec. IV D we will return to this issue when we try to systematically improve the numerical treatment to resolve such tiny energy differences.

C. Total-energy studies for Ce in the experimentally reported high pressure phases with optimized structural parameters

In a third set of calculations, SET3, we have performed total-energy calculations as a function of volume for Ce in the experimentally observed phases using the optimized structural parameters obtained from the SET2 calculations. For the fcc structure 145 k points in the IBZ was used and for the bct structure the theoretically optimized $c/a=1.6697$ with 163 k points in the IBZ was used. For the α-U structure we have used the theoretically optimized structural parameters; $a/b=0.5143$, $c/b=0.8745$, and the internal parameter $y=0.105$ using 150 k points in the IBZ of the C-face-centered orthorhombic lattice. For the $C2/m$ lattice, the theoretically optimized structural parameters are $a/b=1.8151$, $c/b=1.8087$, and $\beta=112.351°$ and the position parameters $z=0.2517$ and $x=0.2618$ were used in combination with 150 k points in the IBZ. As our structural optimization for the body-centered monoclinic lattice always gives fcc or bct structural parameters, we have used the experimental[26] $a/b=0.988$, $c/b=1.5213$, and $\beta=91.91°$ with 150 k points in the IBZ of the body-centered monoclinic lattice. The converged potential as well as energy parameters obtained at 19.7 Å^3/atom for these five different structures are used to calculate the density of states (DOS).

In order to elucidate the relative stability between the various experimentally reported high pressure phases of Ce, the energy difference between the low-pressure fcc phase and the suggested high-pressure phases obtained from our SET3 calculations are shown in Fig. 9. From this figure we notice that both the $C2/m$ as well as the $I2/m$ structures are energetically in the neighborhood to the fcc and bct structures at low pressures. Furthermore, both these structures become more stable at high pressures than the fcc structure. However, before the fcc→$C2/m$ or $I2/m$ structural transitions, Ce is stabilized by adopting the bct phase at high pres-

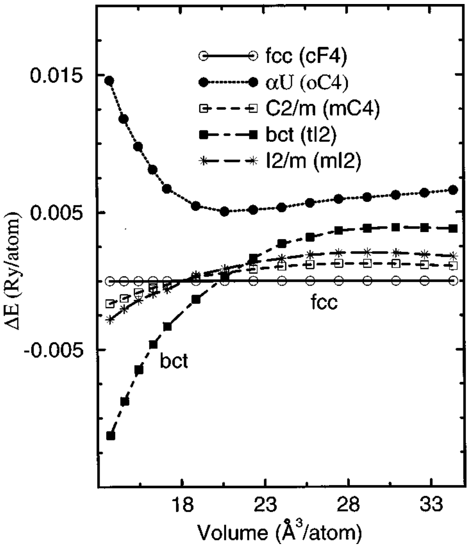

FIG. 9. The total-energy curves for the high-pressure phases of Ce relative to the α(fcc) phase as obtained from SET3 calculations.

sures, as shown in Fig. 9. Also, we conclude once more that the experimentally often reported α-U structure and the hcp structure are never close to the ground-state energy in the volume interval studied here. The α-U structure can be viewed as a highly distorted version of the fcc structure. Thus both in the $C2/m$ structure as well as in the α-U structure the atom positions are displaced from the fcc structure. Our structural optimizations show that the atom displacements in the $C2/m$ structure are smaller than they are in the α-U structure. Up to the fcc→bct structural transition point the total energy difference between the fcc and α-U structures is almost constant. Below this volume, due to the competition between the Madelung term and the $4f$ one-electron energy term, the structural energy difference between fcc and α-U structures increases (Fig. 9) in favor of the symmetric fcc phase.[9]

D. Total-energy studies of Ce in the fcc, bct, and $C2/m$ structures using a common $C2/m$ lattice

Our LDA calculations show that the energy difference between the fcc and the $C2/m$ structure of Ce is less than one mRy. Systematic computational errors between the different structures, due to differences in truncation of Fourier components, k-point convergence, and so on makes it hard to resolve very small energy differences. In order to circumvent this problem we have represented the fcc as well as the bct lattice in a common $C2/m$ lattice by the following procedure, namely, so that the $C2/m$ lattice can be viewed as a small distorted version of the bct/fcc lattice. For fcc as well as for bct the atomic position parameters x and z are 0.25 in the $C2/m$ lattice. Furthermore, the fcc structure can be viewed as a bct structure with $c/a=\sqrt{2}$. The c/b as well as a/b ratio for the fcc and bct structures in the $C2/m$ lattice [i.e., $(a/b)_{\text{fcm}}$ and $(a/b)_{\text{fcm}}$] can be derived from their c/b values in the bct lattice through the following relation:

$$(c/b)_{\text{fcm}}=(a/b)_{\text{fcm}}=\sqrt{1+(c/b)^2_{\text{bct}}}. \qquad (1)$$

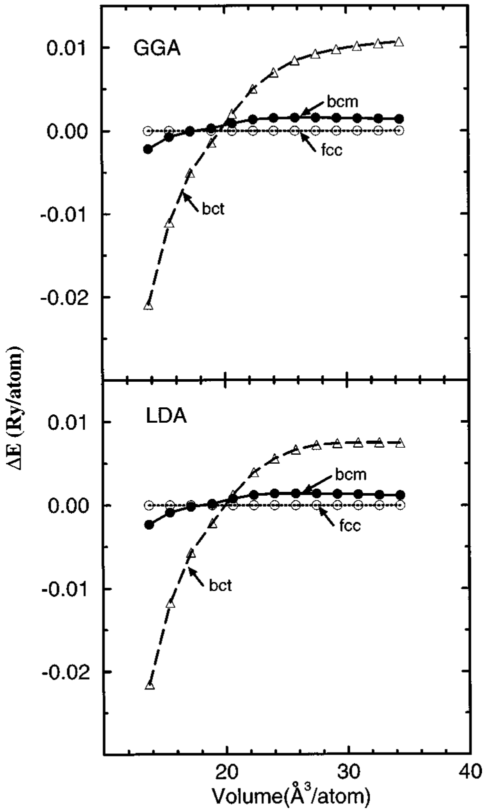

FIG. 10. The relative total-energy curves with respect to the fcc structure for the generalized gradient (GGA) and local-density (LDA) approximations to the density functional. The different structures are represented by a common $C2/m$ lattice, i.e., the results are obtained from SET4 calculations.

The values of the angle β for the fcc as well as the bct structures in the $C2/m$ lattice can be obtained from their c/b value in the bct lattice,

$$\beta=\cos^{-1}\left(1-\frac{4}{\left(\frac{\sqrt{2}}{(c/b)_{\text{bct}}}\right)^2+2}\right). \qquad (2)$$

The atom positions, a/b, c/b, and the β values for the fcc, bct, and $C2/m$ in the $C2/m$ lattice used in our fourth set of calculations, SET4, are given in Table I. There is only one atom/primitive cell in both the fcc as well as the bct structures of Ce, while there are two atoms/primitive cell involved in the calculations for both the fcc and the bct structures in the $C2/m$ settings given in Table I. Using 150 k points in the IBZ of the $C2/m$ lattice, total-energy calculations as a function of volume for the fcc, bct, and $C2/m$ structures have been performed. In addition, it has recently been shown that nonlocal corrections to the local density approximation (LDA), by means of the generalized gradient approximation[35] (GGA) for the exchange and correlation functional, substantially improve the results for bulk properties of f-electron systems.[36] For that reason the GGA, as implemented by Söderlind *et al.*,[36] has also been used for the fcc, bct, and $C2/m$ structures in the common $C2/m$ lattice.

Using the mentioned computational prescriptions we have calculated the LDA total-energy difference between the fcc,

$C2/m$, and bct structures. The results are shown in the lower panel of Fig. 10. As can be seen, the fcc structure is more stable than the $C2/m$ phase up to the pressure where the fcc →bct structural transition takes place. The earlier calculations[36] show that the GGA considerably improve the ground-state properties of f-electron systems compared with that obtained from LDA calculations. The equilibrium volume for the α phase obtained from LDA calculations is 23.155 Å^3/atom, from GGA calculation it is 25.726 Å^3/atom. The latter is comparable to the experimental value of 28.521 Å^3/atom. Our calculated LDA and GGA equilibrium volumes are found to be in good agreement with the value of 22.74 and 26.05 Å^3/atom, respectively, obtained by Söderlind *et al.*[36] The small difference between these two results is mainly due to the k-point effect. Söderlind *et al.* used 60 k points in the IBZ of the fcc lattice. We have used 150 k points in the IBZ of the $C2/m$ lattice in our present study. The GGA total-energy difference between the fcc, bct, and C2/m structures are shown in the upper panel in Fig. 10. Even though the GGA calculations substantially improve the equilibrium volume of the α phase the relative stabilities between fcc, bct, and $C2/m$ structure are not changed significantly.

E. Density of states studies and discussion

In order to gain insight into the electronic structure and phase stability of Ce in the different high-pressure phases, the angular momentum decomposed density of states (DOS) in the experimentally reported high-pressure phases are shown in Fig. 11 for a volume close to the fcc-to-bct structural transition volume. The interesting aspect of this figure is the position of the Fermi energy, E_F on a shoulder of a van Hove–like peak in the DOS curve in the fcc phase and in a pseudogap region in all the other structures. A strong correlation is observed[37] between structural stability and the position of the Fermi level in the DOS curve in binary alloys: that is, if E_F falls in a pseudogap that separates bonding states from antibonding/nonbonding states in a particular structure, the system will gain stability. From the DOS curves we can thus get a qualitative explanation for why distorted phases are favored in Ce at lower volumes. A compression of Ce metal increases the f occupation so that the symmetry breaking mechanism, provided by the f states,[9,32,38] increases in strength and outweighs the Madelung and overlap repulsion, which favor high-symmetry structures. This analysis may help in understanding that at compressed volumes Ce should stabilize in a distorted structure. However, it is impossible to explain from the DOS curves alone which of the different distorted structures should be stable. Also, the occupation numbers at a given volume are approximately the same in all the relevant structures, as shown in Table II. Thus, the intricate information about which of the different distorted structures will be stable can only be obtained after considering all mechanisms that may stabilize one structure over the other. In short, after an accurate evaluation of the density-functional energy.

It is recognized[39–41] that topological changes of the Fermi surfaces can lead to anomalies in phonon frequencies and in some cases to phonon softening and structural transitions. From a Rietveld analysis of the atomic displacements of Pr atoms in its distorted fcc phase, Hamaya *et al.*[42] suggested that the softening of the TA phonon mode at the zone-boundary point L in the Brillouine zone of the fcc lattice drives the fcc → distorted-fcc phase transition. As a result of softening of the lattice, the electron-phonon coupling constant will become enhanced and superconductivity will often appear or to be enhanced. This may be one of the reasons for the experimentally[16] observed pressure induced superconductivity in Ce. It is interesting to note that, if the lattice becomes softened, the atoms will displace their positions

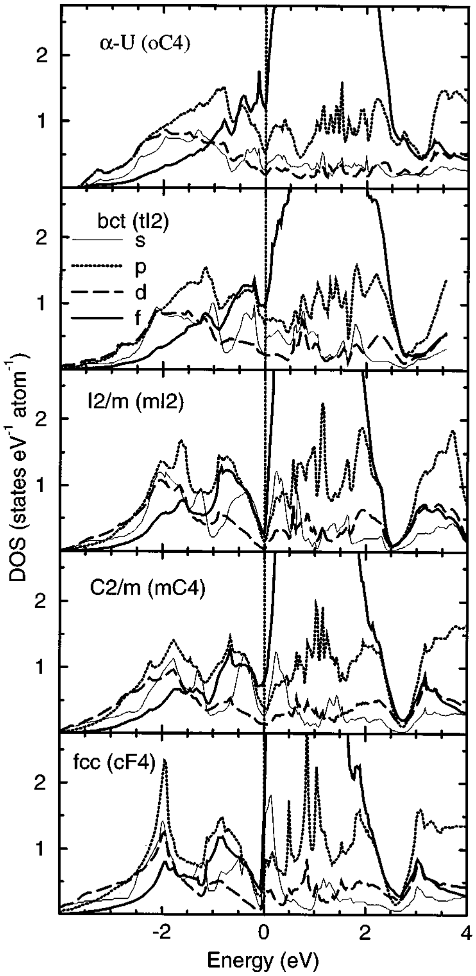

FIG. 11. The angular momentum decomposed density of states curves for Ce in the fcc, bct, $C2/m$, $I2/m$, and α-U structures at the volume 19.7 Å^3/atom.

TABLE II. Calculated occupation numbers (electrons/atom) for Ce in the experimentally reported five different high-pressure phases at an atomic volume 19.7 Å^3 and with a 1.18 Å muffin-tin radius, where ''int'' means occupation number in the interstitial region.

Phase	s	p	d	f	int
α(fcc)	1.878	4.687	0.845	1.019	3.567
$\alpha'(\alpha-U)$	1.868	4.695	0.882	1.016	3.534
α''(I)($I2/m$)	1.876	4.689	0.840	1.017	3.573
α''(II)($C2/m$)	1.877	4.688	0.848	1.018	3.565
ϵ(bct)	1.872	4.689	0.855	1.020	3.558

easily. This may also be the reason for the appearance of metastable phases at high pressure. It is worth mentioning that the structural instabilities in actinide elements[38] have recently been linked to the presence of degenerate pdf hybridized states near the Fermi level and that this degeneracy generally causes Jahn-Teller/Peierls–type of distortions.

At ambient pressure it is known from theory[44] that α-Ce has a small tetragonal shear constant. This particular elastic constant is relevant for the phase transition from fcc to bct since it corresponds exactly to the deformation (tetragonal) that transforms the fcc (c/a$=\sqrt{2}$) lattice into a bct (general c/a) lattice (i.e., along the Bains path). A small tetragonal shear constant (C') suggests that it is energetically easy to change the c/aratio, i.e., an fcc→bct phase transition is expected to be close in this situation. A continuous fcc to bct, i.e., a second order phase transition, occurs when $C'\rightarrow 0$. Our LDA as well as GGA calculations show that there is $\sim$1% volume collapse at the fcc-to-bct structural transition point, which is consistent with recent experimental studies. The pressure for the fcc-to-bct structural transition obtained from our LDA calculations is 11.5 GPa, while our GGA calculations give a slightly higher value of 14.5 GPa. These numbers are comparable with the experimental transition pressures reported to occur between 10 the 13 GPa. The zero-pressure bulk modulus obtained from the LDA total-energy curve fitted to the Birch-Murnaghan equation of state for fcc Ce is 58.8 GPa and for bct Ce it is 58.6 GPa. The corresponding value, obtained from the GGA calculation, for the fcc structure is 42.9 GPa and for the bct structure it is 42.7 GPa.

V. CONCLUSIONS

We have investigated the experimentally reported intermediate pressure phases $[\alpha', \alpha''(\mathrm{I}),\alpha''(\mathrm{II})]$ together with the phases at ambient condition (fcc) and high pressure (bct) of Ce metal. Our structural optimization of the different structures yields data in good agreement with experiment. When comparing the different structural energies with each other we obtain a fcc→bct structural transition at a volume of 20.2 Å^3/atom. In a volume interval close to this transition we find that the fcc, bct, α''(I) and α''(II) structures are within 0.5 mRy/atom of each other. Unfortunately these energy differences are close to the limits for our total-energy resolution, although efforts have been made to minimize the numerical noise in the calculations. Our data are nevertheless consistent with the fact that certain experiments observe the α''(I) structure as an intermediate pressure phase whereas other experiments report the α''(II) structure. We have also shown that the presence of the f electrons as chemically binding itinerant states is reflected indirectly in the distorted intermediate pressure phases as well as in the absence of a stability of the ω structure.

Our c/a optimization as a function of volume in the bct lattice shows a metastable phase intermediate between the fcc and the bct structures with $c/a=1.51$. This phase is identified as the $C2/m$ structure. The structural optimizations of the body-centered monoclinic phase always yield the fcc or the bct structures depending upon the volume we consider. This indicates that there is only a low possibility that the body-centered monoclinic phase is stabilized in the P-T phase diagram of Ce and this is in fact consistent with recent experimental results.[27] The optimized structural parameters for the $C2/m$ and the α-U structures are found to be in good agreement with the experimental values. However, the α-U structure is much higher in energy than the $C2/m$ structure over the whole volume range, which suggests that it is easier to stabilize the $C2/m$ structure than the α-U structure at high pressures. This is also consistent with the experimental studies in the sense that the α-U phase of Ce is only stabilized above $\sim$ 400 K. Our calculations show that the high-pressure structural transition away from the fcc phase in Ce involves an electronic topological transition and, accordingly, one could expect phonon softening near the phase transition. Further, the phonon softening may be the reason for the appearance of pressure-induced superconductivity in Ce. The experimentally reported intermediate pressure phases such as α-U, $C2/m$, and $I2/m$ are found to be metastable phases and may be stabilized only at high temperatures. More experimental high-pressure studies at low temperatures are needed in order to confirm our expectations. In conclusion, the fcc→$C2/m$→bct structural sequence as a function of pressure is energetically more favorable at low temperature for Ce than the fcc →α-U→bct sequence.

ACKNOWLEDGMENTS

We are thankful for financial support from the Swedish Natural Science Research Council and for support from the Materials Science Consortium No. 9. P.R. wishes to acknowledge P. Blaha for his help in the initial stages of this work and L. Fast and A. Delin for many enlightening discussions. Part of the work was performed under the auspices of the U.S. Department of Energy.

---

[1] P. W. Bridgeman, Proc. Am. Acad. Arts. Sci. **62**, 207 (1927).

[2] K. A. Gshneidner, Jr. and L. Eyring, *Handbook on the Physics and Chemistry of Rare Earths* (North-Holland, Amsterdam, 1979), Vol. I.; B. Johansson and A. Rosengren, Phys. Rev. B **11**, 2836 (1975).

[3] K. A. Gshneidner, Jr., R. O. Elliott, and R. R. McDonald, J. Phys. Chem. Solids **23**, 555 (1962).

[4] W. H. Zachariasen, (unpublished) quoted in A. W. Lawson, and T. Y. Tang, Phys. Rev. **76**, 301 (1949); L. Pauling, J. Am. Chem. Soc. **69**, 542 (1947).

[5] J. W. Allen and R. M. Martin, Phys. Rev. Lett. **49**, 1106 (1982); J. W. Allen and L. Z. Liu, Phys. Rev. B **46**, 5047 (1992).

[6] B. Johansson, Philos. Mag. **30**, 469 (1974).

[7] I. Sandalov, O. Hjortstam, B. Johansson, and O. Eriksson, Phys. Rev. B **51**, 13 987 (1995).

[8] W. E. Pickett, A. J. Freeman, and D. D. Koelling, Phys. Rev. B **23**, 1266 (1981); D. Glötzel, J. Phys. F **8**, L163 (1978); B. I. Min, H. J. F. Jansen, T. Oguchi, and A. J. Freeman, Phys. Rev. B **34**, 369 (1986); O. Eriksson, M. S. S. Brooks, and B. Johansson *ibid.* **41**, 7311 (1990).

[9] J. M. Wills, O. Eriksson, and A. M. Boring, Phys. Rev. Lett. **67**, 2215 (1991); O. Eriksson, J. M. Wills, and A. M. Boring, Phys. Rev. B **46**, 12 981 (1992).

[10] E. Wuilloud, H. R. Moser, W. D. Schneider, and Y. Baer, Phys-.Rev. B **28**, 7354 (1983).

[11] P. Fulde, J. Keller, and G. Zwicknagl, Solid State Phys. **41**, 1 (1988).

[12] A. M. Boring, R. C. Albers, O. Eriksson, and D. D. Koelling, Phys. Rev. Lett. **68**, 2652 (1992).

[13] B. Brandow, Adv. Phys. **26**, 651 (1977).

[14] Z. Szotek, W. M. Temmerman, and H. Winter, Phys. Rev. Lett. **72**, 1244 (1994); A. Svane *ibid.* **72**, 1248 (1994); A. Svane, Phys. Rev. B **53**, 4275 (1996).

[15] B. Johansson, I. A. Abrikosov, M. Aldén, A. V. Ruban, and H. L. Skriver, Phys. Rev. Lett. **74**, 2335 (1995).

[16] Jörg Wittig, Phys. Rev. Lett. **21**, 1250 (1968).

[17] E. Franceschi and G. L. Olcese, Phys. Rev. Lett. **22**, 1299 (1969).

[18] D. B. McWhan, Phys. Rev. B **1**, 2826 (1970).

[19] F. H. Ellinger and W. H. Zachariasen, Phys. Rev. Lett. **32**, 773 (1974).

[20] Ph. Schaufelberger, J. Appl. Phys. **47**, 2364 (1976).

[21] S. Endo, H. Sasaki, and T. Mitsui, J. Phys. Soc. Jpn. **42**, 882 (1977).

[22] W. H. Zachariasen and F. H. Elliger, Acta Crystallogr., Sect. A: Cryst. Phys., Diffr., Theor. Gen. Crystallogr. **33**, 155 (1977).

[23] W. H. Zachariasen, Proc. Natl. Acad. Sci. USA **75**, 1066 (1978).

[24] J. Staun Olsen, L. Gerward, U. Benedict, and J. P. Itié, Physica **133B**, 129 (1985).

[25] S. K. Sikka and V. Vijayakumar, Physica B **144B**, 23 (1986).

[26] G. Gu, Y. K. Vohra, and K. E. Brister, Phys. Rev. B **52**, 9107 (1995).

[27] M. I. McMahon and R. J. Nelmes, Phys. Rev. Lett. **78**, 3884 (1997).

[28] Y. C. Zhao and W. B. Holzapfel, J. Alloys Compd. **246**, 216 (1997).

[29] H. L. Skriver, Phys. Rev. B **31**, 1909 (1985).

[30] O. K. Andersen, Phys. Rev. B **12**, 3060 (1975).

[31] J. M. Wills (unpublished); J. M. Wills and B. R. Cooper, Phys. Rev. B **36**, 3809 (1987); D. L. Price and B. R. Cooper, *ibid.* **39**, 4945 (1989).

[32] J. M. Wills, O. Eriksson, and A. M. Boring, Phys. Rev. Lett. **67**, 2215 (1992); O. Eriksson, P. Söderlind, and J. M. Wills, Phys. Rev. B **45**, 12 588 (1992); J. M. Wills and O. Eriksson, *ibid.* **45**, 13 879 (1992).

[33] D. J. Chadi and M. L. Cohen, Phys. Rev. B **8**, 5747 (1973); S. Froyen, *ibid.* **39**, 3168 (1989).

[34] R. Ahuja, J. M. Wills,. B. Johansson, and O. Eriksson, Phys. Rev. B **48**, 16 269 (1993).

[35] J. P. Perdew, J. A. Chevary, S. H. Vosko, K. A. Jackson, M. R. Pederson, and D. J. Singh, Phys. Rev. B **46**, 6671 (1992).

[36] P. Söderlind, O. Eriksson, B. Johansson, and J. M. Wills, Phys. Rev. B **50**, 7291 (1994); *ibid.* **52**, 13 169 (1995).

[37] J.-H. Xu, T. Oguchi, and A. J. Freeman, Phys. Rev. B **35**, 6940 (1987); J.-H. Xu and A. J. Freeman, *ibid.* **40**, 11 927 (1989); , J. Mater. Res. **6**, 1188 (1991); P. Ravindran, G. Subramoniam, and R. Asokamani, Phys. Rev. B **53**, 1129 (1996).

[38] P. Söderlind, O. Eriksson, B. Johansson, J. M. Wills, and A. M. Boring, Nature (London) **374**, 524 (1995).

[39] W. A. Grosshans, Y. K. Vohra, and W. B. Holzapfel, Phys. Rev. Lett. **49**, 1572 (1982).

[40] L. Dagens, J. Phys. F **8**, 2093 (1978).

[41] J. E.Schirber, in *High Pressure Science and Technology*, edited by K. D. Timmerhaus and M. S. Barber (Plenum, New York, 1979), Vol. 1, p. 130.

[42] N. Hamaya, Y. Sakamoto, H. Fujihisa, Y. Fujii, K. Takemura, T. Kikegawa, and O. Shimomura, J. Phys.: Condens. Matter. **5**, L369 (1993).

[43] J. D. Becker, J. M. Wills, L. Cox, and B. R. Cooper, Phys. Rev. B **54**, R17 265 (1996).

[44] P. Söderlind, O. Eriksson, J. M. Wills, and A. M. Boring, Phys. Rev. B **48**, 9306 (1993).